Nepenthes Pitcher Inspired Anti-Wetting Silicone Nanofilaments Coatings: Preparation, Unique Anti-Wetting and Self-Cleaning Behaviors

Junping Zhang, Aiqin Wang, and Stefan Seeger*

Nepenthes **pitcher inspired anti-wetting coatings, fluoro-SNs/Krytox, are successfully fabricated by the combination of fluoro-silicone nanofilaments (fluoro-SNs) and Krytox liquids, perfluoropolyethers. Fluoro-SNs with different microstructure are grown onto glass slides using trichloromethylsilane by simply repeating the coating step, and then modified with 1H,1H,2H,2H-perfluorodecyltrichlorosilane. Subsequently, the Krytox liquid is spread on the fluoro-SNs coatings via capillary effect. The fluoro-SNs/Krytox coatings feature ultra-low sliding angle for various liquids, excellent stability, and transparency. The sliding speed of liquid drops on the fluoro-SNs/Krytox coating is obviously slower than on the lotus inspired superhydrophobic and superoleophobic coatings, and is controlled by composition of the coating (e.g., morphology of the fluoro-SNs, type of Krytox and its thickness) and properties of the liquid drops (e.g., density and surface tension). In addition, the self-cleaning property of the fluoro-SNs/Krytox coating is closely related to properties of liquid drops and dirt.**

1. Introduction

Inspired by the self-cleaning property of lotus leaf, superhydrophobic surfaces develop very quickly.[1] Now, it is well known that the combination of proper surface roughness and materials with low surface energy is a successful way to prepare superhydrophobic surfaces.[2] However, it is very challenging to create superoleophobic surfaces that resist wetting of non-polar liquids because of their low surface tension, for example, *n*-hexadecane (27.5 mN m^{-1}) and *n*-decane (23.8 mN m^{-1}), compared to water (72.8 mN m^{-1}). With the experience of designing superhydrophobic surfaces, many groups have tried various techniques to create superoleophobic surfaces.[3,4] However, droplets of non-polar liquids often have high contact angles (CA ≈150°) on most of the reported superoleophobic surfaces but adhere on the surface and cannot roll down.[4] This means these surfaces have no self-cleaning property once encountered non-polar liquids. In fact, materials of both very low surface tension and special microstructure are necessary in order to weaken the interaction between droplets and surfaces, which is very important for non-polar liquids to roll down.[5] Until now, only a few studies reported very low sliding angle (SA <10°) for non-polar liquids by using fluoro-POSS with very low surface tension or by introducing some special patterns like "overhang structures", "re-entrant surface curvatures", candle soot, and silicone nanofilaments (SNs).[6,7] For example, mushroom-like micropillar arrays were used to prepare superomniphobic surfaces with high transparency by Suh and co-workers.[6f] However, these superoleophobic surfaces still have many problems such as low mechanical stability, failure under pressure, and high production cost, which seriously restrict their potential applications.

To address these problems, Jiang and colleagues developed a feasible strategy in 2009 to create low-adhesive superoleophobic interfaces inspired by fish scales.[8] Aizenberg and co-workers designed slippery liquid-infused porous surfaces (SLIPS) inspired by *Nepenthes* pitcher.[9] The SLIPS show overwhelming properties over all the state-of-the-art superoleophobic coatings, according to the authors' statement, in many respects, for example, repel various liquids and quick self-healing after physical damage. These new anti-wetting surfaces generate extensive attention[10,11] and show promising applications in many fields including anti-icing and anti-biofouling.[12] The previous studies on these new coatings are encouraging, but additional research is needed before applications will emerge.[10] The information we have got about them is just the tip of the iceberg in comparison with the well developed superhydrophobic coatings. For example, there is no difference in SA for all the investigated liquids on SLIPS.[9] However, we found that the sliding speed of liquid droplets on the *Nepenthes* pitcher inspired coatings is different from each other, and is obviously slower than on the traditional lotus-inspired superhydrophobic and superoleophobic coatings.

Here, we report fluoro-SNs/Krytox anti-wetting coatings inspired by *Nepenthes* pitcher on the basis of our work about

---

Prof. J. P. Zhang, Prof. A. Q. Wang
Center of Eco-material and Green Chemistry
Lanzhou Institute of Chemical Physics
Chinese Academy of Science
730000, Lanzhou, P. R. China
E-mail: jpzhang@licp.cas.cn
Prof. S. Seeger
Physikalisch-Chemisches Institut
Universität Zürich Irchel
8057, Zürich, Switzerland

DOI: 10.1002/adfm.201301481

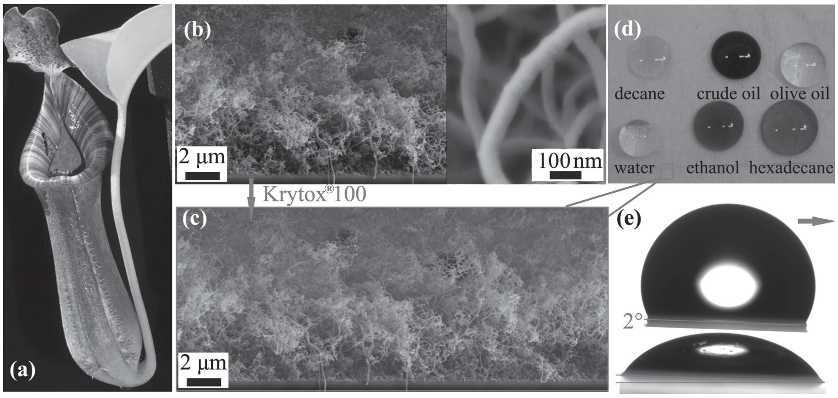

Figure 1. Preparation of the fluoro-SNs/Krytox anti-wetting coatings. a) Image of *Nepenthes* pitcher, SEM (titled view, 90°) of b) fluoro-SNs1 and c) fluoro-SNs1/Krytox 100 coatings on glass slides, d) various liquids on the fluoro-SNs1/Krytox 100 coating, and e) optical graphs of water (up) and n-decane (down) drops (10 µL) on the fluoro-SNs1/Krytox 100 coating. The water and ethanol drops in (d) were colored with methylene blue (MB). The n-hexadecane and n-decane drops in (d) were colored with oil red O (OR).

SNs (**Figure 1**a–c).[7,13] The coatings feature ultra-low sliding angle for various liquids, excellent stability, and transparency. The sliding speed of liquid drop and the self-cleaning property can be controlled by composition of the coating, properties of liquid drop and dirt.

2. Results and Discussion

2.1. Preparation of the Fluoro-SNs/Krytox Anti-Wetting Coatings

The fluoro-SNs/Krytox coatings were prepared by the combination of fluoro-SNs coated glass slide and Krytox liquid, a perfluoropolyether. Firstly, SNs with different microstructure were grown onto glass slides using trichloromethylsilane (TCMS) by simply repeating the coating step. Subsequently, the SNs were modified with 1*H*,1*H*,2*H*,2*H*-perfluorodecyltrichlorosilane (PFDTS) to get fluoro-SNs. This is important to decrease the surface tension of SNs and match with the Krytox liquid. Finally, the Krytox liquid was spread on the fluoro-SNs coated glass slide via capillary effect. Thus, the lotus-inspired superoleophobic fluoro-SNs coating acting via heterogeneous liquid/solid interface was converted to the pitcher-inspired anti-wetting fluoro-SNs/Krytox coating acting via homogeneous liquid/liquid interface.

The hydrolysis of TCMS in toluene with a water concentration of 120 ppm generates a large amount of SNs on the surface of glass slide (Figure 1b and Figure S1, Supporting Information). The SNs are 50–90 nm in diameter, several micrometers in length and about 9 µm in thickness. The rough topography of the SNs coating and the preferred presence of the methyl groups at the surface of SNs generate a superhydrophobic surface ($CA_{water} \approx 170°$ and $SA_{water} \approx 2°$). This surface can be easily wetted by the Krytox liquid, but cannot hold it in place owing to their big surface tension difference. The SNs must be modified with fluorochemicals to decrease the surface tension in order to firmly hold the Krytox liquid. Here, the SNs were treated with O_2-plasma to convert the hydrophobic methyl groups on the surface of SNs to hydrophilic hydroxyl groups while keeping the SNs skeleton intact, and then modified with PFDTS to get the fluoro-SNs. Once the Krytox liquid was dropped onto the fluoro-SNs coating, it quickly wetted and spread out on the whole fluoro-SNs coating via capillary effect. Consequently, the Krytox liquid was firmly held among the fluoro-SNs and the anti-wetting fluoro-SNs/Krytox coating was fabricated.

2.2. Anti-Wetting Behaviors of the Fluoro-SNs/Krytox Coatings

The fluoro-SNs/Krytox coatings feature ultra-low SA for various liquids (e.g., water, *n*-hexadecane and *n*-decane), excellent stability (e.g., mechanical, chemical, and environmental) and transparency (Figure 1d,e). On the fluoro-SNs/Krytox coating, the sliding speed of liquids is evidently slower than on the traditional superhydrophobic and superoleophobic coatings (Movie S1, Supporting Information), and is obviously different from each other. In this section, various factors influencing the anti-wetting behaviors (sliding speed, SA and CA) of the fluoro-SNs/Krytox coatings were investigated.

The microstructure of fluoro-SNs and the thickness of the Krytox layer have influences on CA and SA, especially sliding speed, of water and *n*-decane (**Figure 2** and Figure S2, Supporting Information).

An evident decrease in CA of water and *n*-decane was observed once the fluoro-SNs1 coating (CA = 162.5° for a 5 µL *n*-decane drop[7]) was converted to the fluoro-SNs1/Krytox100 coating. A slight decrease in CA was recorded with increasing thickness of the Krytox100 layer from 5 µm to 10 µm, and then remained constant. The fluoro-SNs coating (≈9 µm in thickness) should be completely covered by the Krytox100 layer (≥10 µm). Or else, the exposed wetted fluoro-SNs could interact with the water and *n*-decane drops, and made them difficult to roll down the surface. Similar to the variation of CA, SA remains very low when the Krytox100 layer is over 10 µm. These results are consistent with Aizenberg and co-workers' report.[9] However, obviously slower sliding speed of liquid drops was observed on the fluoro-SNs/Krytox coating compared to the fluoro-SNs coating. As is well known, liquid droplets could roll off a tilted lotus-inspired superhydrophobic or superoleophobic surface in the twinkling of an eye. However, the liquid drops need a few seconds or even a few minutes to roll off a wafer scale, for example, 40 mm, fluoro-SNs/Krytox coating. This indicates the stronger interaction between liquid drops and the fluoro-SNs/Krytox coating, originating from the friction and adhesion forces between them. Different from CA and SA, the sliding speed increases evidently with increasing thickness of the Krytox100 layer to 25 µm (Figure 2a). For example, the sliding speed of *n*-decane increases from 2.13 mm s^{-1} to 8.12 mm s^{-1} on the fluoro-SNs2/Krytox100 surface with increasing the thickness of the Krytox100 layer from 10 µm to

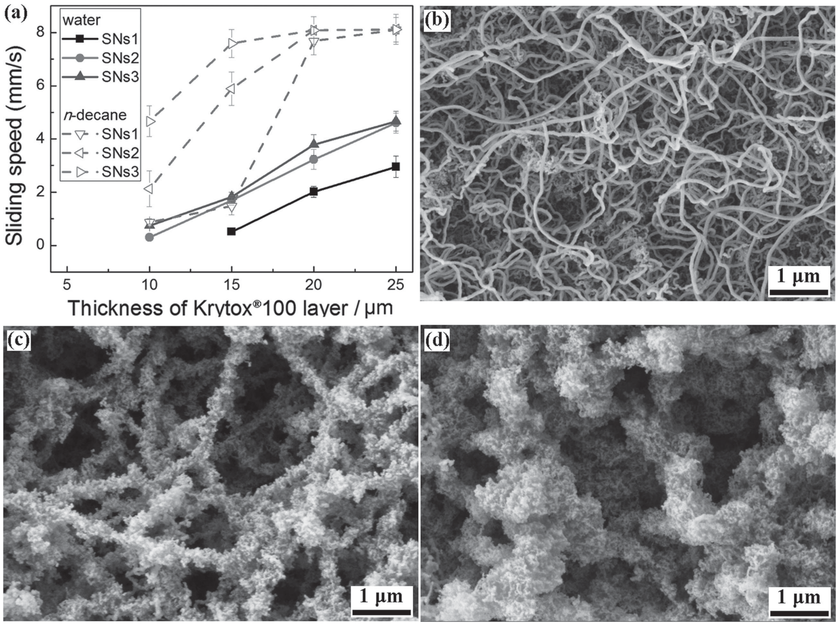

Figure 2. a) Variation of sliding speed (on 10° tilted sample) of water and *n*-decane drops (10 μL) with structure of SNs and thickness of Krytox100 layer on the fluoro-SNs/Krytox100 coatings. SEM images of b) SNs1, c) SNs2, and d) SNs3.

25 μm. Drops of the same liquids cannot mix with each other with further increase in thickness to 30 μm. This means there is an immiscible layer between them and formation of cloaked drops (Figure S3, Supporting Information). The smooth Krytox100 layer could be deformed by gravity of drops, surface tension and interaction with drops, which makes it possible for the contact of liquid drops with the fluoro-SNs beneath the thin Krytox100 layer, for example, 10 μm (Figure S4, Supporting Information). With increasing the thickness of Krytox100 layer, the contact between drops and fluoro-SNs was avoided, and then the increased sliding speed was observed. So, the thickness of Krytox100 layer above the fluoro-SNs coating plays an important role in influencing the sliding speed. A Krytox100 layer with a thickness of 20–25 μm is necessary to ensure excellent anti-wetting performance (high sliding speed and low SA) of the fluoro-SNs/Krytox100 coatings.

The morphology and density of the fluoro-SNs coating can be controlled by repeating the TCMS coating and O_2-plasma treatment steps (Figure 2b–d). TCMS prefers to anchor onto the surface of O_2-plasma treated SNs rather than forming new SNs. Thus, the density and roughness of the SNs coating are in the order of SN1<SN2<SN3, but the thickness remains constant (Figure S5, Supporting Information). No change in CA of water and *n*-decane was observed by varying microstructure of the fluoro-SNs coating (Figure S2, Supporting Information). Their influence in SA was only observed at low thickness (≤10 μm) of the Krytox100 layer. The sliding speed increases with increasing the coating cycles (Figure 2a), especially at lower thickness of the Krytox100 layer and for *n*-decane. This is because the space in the fluoro-SNs coating to hold Krytox100 is in the order of SN1>SN2>SN3. Thus, the thickness of Krytox100 layer above the fluoro-SNs coating increases with increasing the coating cycles, which facilitates quick movement of the liquid drops.

Liquid drops can move on a tilted surface via rolling and/or sliding motions depending on the forces and force moments loaded on them. No rolling motion was observed for all the liquids investigated on the fluoro-SNs/Krytox coating when the tilting angle ≤10°. Considering a condition (e.g., drops with low CA on a slightly tilted surface) without rolling, the liquid drop can move via sliding on a surface only when F_1 (parallel component of gravity) $\geq f$ (friction force between liquid drop and coating) (**Figure 3**a).[14] F_1 is determined by the gravity (density and volume) of liquid drop and the tilting angle. f should relate to physical properties of the liquid drop (e.g., surface tension and polarity), its contact area with the surface (e.g., CA and volume), and properties of the surface (e.g., chemical composition and roughness).[15] For the pitcher-inspired fluoro-SNs/Krytox coatings in this study, f should also relate to viscosity of the Krytox liquid. f is responsible for the deformation of liquid drops on the tilted surface and frequently observed CA hysteresis.

The influences of F_1 and f on SA and sliding speed were studied (Figure 3b–d and Figures S6,S7, Supporting Information). The liquid drop needs to deform the Krytox layer while moving on the fluoro-SNs/Krytox coatings. The increase in viscosity of the Krytox liquid (Table S1, Supporting Information) increases the friction force and makes the Krytox layer difficult to be deformed, which results in increase of SA and evident decrease of sliding speed (Figure S6b, Supporting Information, and Figure 3b). Similar phenomenon was observed by Hozumi and co-workers in improving the mobility of alkane liquid drops using PDMS brush films of different molecular weights.[16] The SA of water and *n*-decane droplets on the fluoro-SNs2/Krytox107 coating is around 12°. So, the water and *n*-decane drops cannot move on the 10° tilted fluoro-SNs2/Krytox107 surface. Krytox107 imparts a more solid-like character to the surface, which provides more resistance to the movement of the probe liquids. The increases in volume of liquid drop and tilting angle could enhance F_1, which is of great benefit to the sliding speed. Consequently, an increase in sliding speed and a decrease in SA (Figure S7b, Supporting Information) were observed by increasing the volume. Similar phenomena also can be seen by increasing the tilting angle.

The CA of all the investigated liquid droplets (Table S2, Supporting Information) on the fluoro-SNs2/Krytox100 coating increases with increasing the surface tension (Figure S8a, Supporting Information). The fluoro-SNs2/Krytox100 coating shows excellent anti-wetting properties. The SA of all the liquid droplets remains below 4° and has no obvious correlation with their surface tension (Figure S8b, Supporting Information). All the liquid droplets, such as various polar and non-polar liquids, commercial oils, and aqueous solutions (Table S3, Supporting Information), could easily roll off the coating.

Interestingly, the sliding speed of liquid drops changes irregularly with their surface tension (Figure S9, Supporting

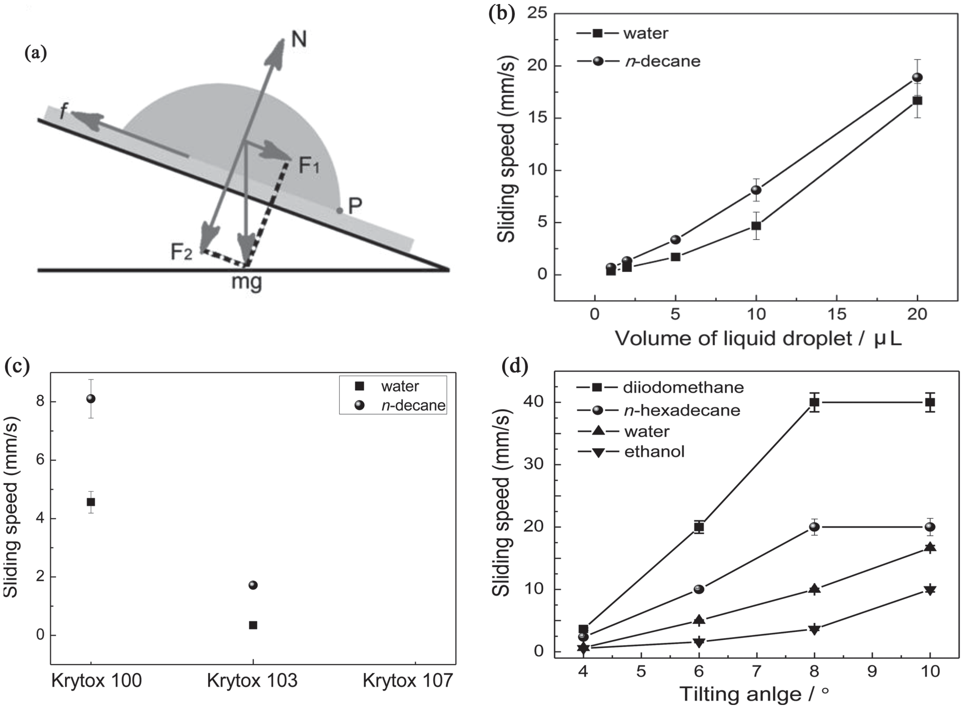

Figure 3. a) The forces loaded on the liquid drop on the titled fluoro-SNs/Krytox coating. Variation of sliding speed with b) kind of Krytox liquid on the 10° tilted fluoro-SNs2/Krytox coatings (10 μL drop), c) volume of liquid drop (on 10° tilted sample), and d) tilting angle (20 μL drop) on the fluoro-SNs2/Krytox100 coating. The thickness of the Krytox layer is 25 μm.

Information). By analyzing the data, it is found that the sliding speed depends on many of the physical parameters of liquid drops, such as density, surface tension, and polarity. Surface tension is not the decisive factor in influencing the sliding speed. The sliding speed is in the order of chloroform and diiodomethane (5.8 mm s^{-1} and 4.3 mm s^{-1}, respectively) > alkanes and arenes > *N, O*-containing liquids (including water) > methanol and ethanol (**Figure 4**a). The obviously higher sliding speed of chloroform and diiodomethane is because of their higher density, which means greater F_1. The F_1 of chloroform and diiodomethane is four to five times of the other liquids with a density of about 1 g mL^{-1}. The higher sliding speed of all the investigated alkanes and arenes than the *N, O*-containing liquids indicates smaller *f* of alkanes and arenes with the fluoro-SNs2/Krytox100 coating since their density are comparable. The reductions in resistance to liquid drop movement are due to the extended chain conformations of Krytox100 with alkanes and arenes compared to the collapsed conformations with the *N, O*-containing liquids.[16] Therefore, sliding speed of alkanes and arenes was higher than that of the *N, O*-containing liquids. Similar result was reported for the SA of alkanes and water on the PDMS coated liquid-like surface.[17] For alkanes and arenes, the sliding speed increases with increasing the surface tension. This is because the increase in surface tension could enhance CA and decrease the contact area of drop with the coating, which is helpful to reduce *f*. In addition, the density of alkanes and arenes gradually increases along with the surface tension by increasing the chain length, which increases F_1 and also contributes to the higher sliding speed. It is difficult to find specific tendency of sliding speed for the *N, O*-containing liquids owing to their big differences in surface tension, viscosity, and density, which mean irregular variation of F_1 and *f*. The lowest sliding speed of methanol and ethanol is attributed to their low density (smaller F_1) and high adhesion force (larger *f*) with the coating. It should be noted that sliding speed measurements are scarce in reports describing wettability of surfaces, especially for lotus-inspired superhydrophobic surfaces and the pitcher-inspired anti-wetting surfaces. The recorded sliding speed is owing to the synergistic effect of F_1 and *f*, which are closely related to the aforementioned factors. For example, water, a frequently used probe liquid, has higher density than *n*-decane, indicating larger F_1. However, the *f* of *n*-decane with the fluoro-SNs2/Krytox100 surface is lower than that of water owing to the extended chain conformations of Krytox100. As a result, a higher sliding speed of *n*-decane was observed in comparison with water.

2.3. Stability of the Fluoro-SNs/Krytox Coatings

In respect of chemical, environmental and mechanical durability of the fluoro-SNs/Krytox coating, a series of experiments have been done under various conditions (Table S4, Supporting Information). The CA and SA of water and *n*-decane droplets on the coating are stable against strong UV light, acidic and basic solutions, ultra-low temperature, and even scratching with a knife, etc. Only ozone treatment slightly decreases the CA of water to 114°. Some of the treatments change sliding

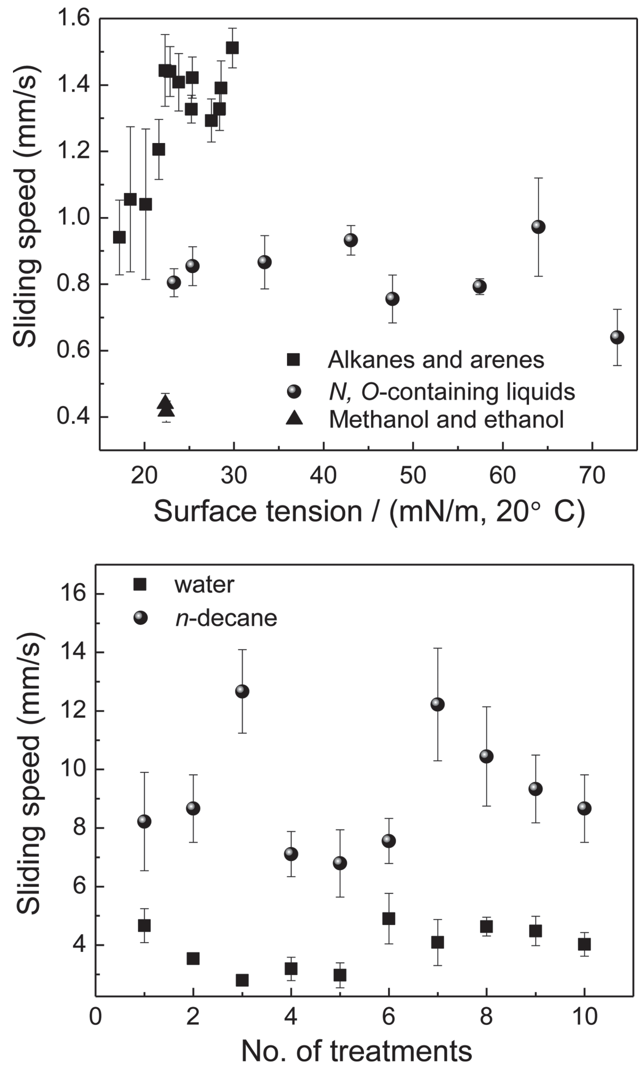

Figure 4. Variation of sliding speed of liquid drop (10 µL) with a) surface tension (4° tilted sample) and b) various treatments (10° tilted sample) on the fluoro-SNs2/Krytox100 coating. The liquids investigated in (a) were shown in Table S2, Supporting Information. The treatments investigated in (b) were shown in Table S4, Supporting Information.

speed of the liquid droplets (Figure 4b). A slight decrease in sliding speed of water droplet was observed after treated by 1 m H_2SO_4 solution, 1 m NaOH solution, ozone and UV light. Even an improvement of sliding speed of *n*-decane was observed after stored at ultra-low temperature (–24 °C and –78 °C) for 24 h or immersed in 1 m NaOH solution for 1 h. Small area of mechanical damage has no obvious influence on the sliding speed of water and *n*-decane droplets. The excellent stability is attributed to the stably adhesion of fluoro-SNs2 for Krytox100 and the fluidic nature of Krytox100. The Krytox100 layer serves as a self-healing coating to rapidly restore the anti-wetting function.

The stability of the surfaces with time was also investigated since the surfaces are based on fluorinated liquids (**Figure 5** and Figure S10, Supporting Information). For the fluoro-SNs2/Krytox100 coating, there is no obvious change in CA, SA, and sliding speed in the first week in ambient conditions. However, gradual increase in CA and SA, and decrease in sliding speed were observed with time extended to three weeks. The sliding speed of water drops decreases from 4.78 mm s^{-1} to 0.37 mm s^{-1} on the 10° tilted surface after storage for 22 d in ambient conditions. This is owing to the evaporation of Krytox100. No change in CA, SA, and sliding speed was detected in three weeks when Krytox103 was used instead of Krytox100. Fluorinated liquids with low volatility should be helpful in maintaining anti-wetting properties of the pitcher-inspired surfaces for a longer period of time.

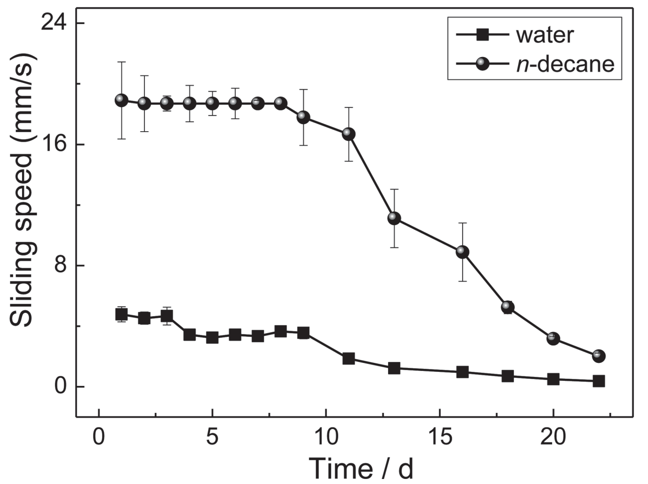

Figure 5. Variation of sliding speed of water (10 µL) and *n*-decane (20 µL) drops with storage time in ambient conditions on the 10° tilted fluoro-SNs2/Krytox100 coating.

2.4. Transparency and Self-Cleaning Behaviors of the Fluoro-SNs/Krytox Coatings

The transition of the lotus-inspired fluoro-SNs2 coating to the pitcher-inspired fluoro-SNs2/Krytox100 coating also evidently improves the transparency (**Figure 6**a). The repeated coating of glass slide with SNs and the subsequent modification with PFDTS decrease the transmittance from 91.2% (bare glass slide) to 51% at 600nm owing to the light scattering at the solid/air interface by the rough fluoro-SNs2 coating. By introducing a layer of flat Krytox100, the light scattering is successfully weakened and the fluoro-SNs2 coated glass slide changes from translucent to transparent. The transmittance of the fluoro-SNs2/Krytox100 coating is close to the bare glass slide in the range of 300–800nm and the transmittance at 600 nm is as high as 89%.

One of the most important motives for researchers to design such bio-inspired surfaces is to use their self-cleaning property. The self-cleaning property of lotus-inspired superhydrophobic and superoleophobic coatings is based on 1) the weak interaction of the coatings with liquid drop and the dirt, and 2) rolling of liquid drop down the coatings. The motion of droplet is determined by the forces and force moments loaded on it.[14] The instantaneous contact point P in Figure 3a can be regarded

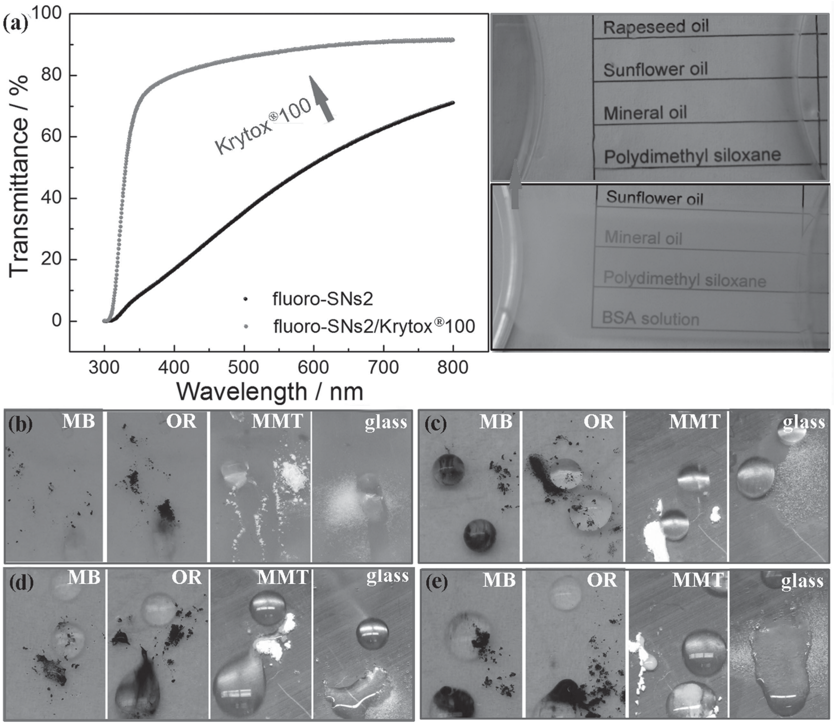

Figure 6. a) Transmittance of the fluoro-SNs2 coating, fluoro-SNs2/Krytox100 coating (25 µm in thickness) and the corresponding digital images. Self-cleaning property of b) the superhydrophobic fluoro-SNs2 coating with water as the liquid, the fluoro-SNs2/Krytox100 coating with c) water, d) *n*-decane, and e) ethanol as the liquids. MB, OR, montmorillonite (MMT), and glass particles were used as the dirt.

as the rolling axis when a tilted drop starts rolling. Among the forces loaded on the droplet, F_1 creates a force moment by acting on the mass center of the droplet. Whereas, the friction force, *f*, acts through the contact point P and thus no force moment is created. When the drop tends to roll, the adhesion force (*M*) between the drop and the surface generates a new force moment which prevents the droplet from rolling.[14] Thus, the drop will 1) slide down when $F_1 > f$, but the force moment of F_1 is less than that of *M*, 2) roll off when $F_1 < f$, but the force moment of F_1 can overcome that of *M*, and 3) roll and slide off simultaneously while $F_1 > f$ and the force moment of F_1 is larger than that of *M*.

The self-cleaning property of the fluoro-SNs2/Krytox100 coating was studied and compared with the fluoro-SNs2 coating (Figure 6 and Movie S2, Supporting Information). All the powdered dirt can be easily removed from the fluoro-SNs2 coating owing to the rolling motion of water on the surface. However, the self-cleaning property of the fluoro-SNs2/Krytox100 coating is closely related to the liquid used and the property of dirt. Water can easily remove hydrophilic MB, MMT and glass particles from the fluoro-SNs2/Krytox100 coating, but difficult to remove OR. *n*-decane is only effective in cleaning OR. Ethanol can remove MB, OR and MMT, but performs badly in cleaning glass particles. The interactions among the liquid drop, dirt and the fluoro-SNs2/Krytox100 coating determine the self-cleaning property.

In addition, the liquid drops tend to slide on the slightly tilted fluoro-SNs2/Krytox100 surface. No rolling motion was observed for all the liquids investigated on the fluoro-SNs2/Krytox100 coating when the tilting angle ≤10°. The composite motion of rolling and sliding was observed only when the coating was quickly tilted for more than 30°. As is well known, the rolling motion of drop is more efficient in cleaning a surface than the sliding motion.[18] A higher CA is of benefit for the rolling off of liquid drops, and then the self-cleaning property.[14,19] The obviously lower CA of liquid drops on the pitcher-inspired surface decreases the force moment of F_1 and increases the force moment of *M* in comparison with the superhydrophobic fluoro-SNs2 coating. Consequently, the self-cleaning property of the pitcher-inspired surfaces depends on the liquid used and the property of dirt, and is obviously different from the lotus-inspired superhydrophobic surfaces.

3. Conclusions

In summary, we have successfully fabricated transparent *Nepenthes* pitcher inspired anti-wetting coatings simply by the combination of fluoro-SNs and Krytox liquid. It was found that the sliding speed of liquid drops is obviously slower than on the lotus-inspired superhydrophobic and superoleophobic coatings. The microstructure of fluoro-SNs, properties of the Krytox layer (e.g., thickness and viscosity) and tilting angle play important roles in influencing the sliding speed. In addition, the sliding speed is also closely related to physicochemical properties of liquid drops, for instance, density, surface tension, and polarity. Moreover, the self-cleaning property of the fluoro-SNs/Krytox coating is closely related to the properties of liquid drop and dirt. We believe that our findings about differences in sliding speed and self-cleaning property between the lotus-inspired and the pitcher-inspired surfaces are helpful in designing new anti-wetting coatings and their practical applications.

4. Experimental Section

Materials: Glass slides (Menzel, Braunschweig, Germany) of 25 mm × 60 mm (1#) were used as the substrates. TCMS (97%, Gelest) and PFDTS ((97%, Gelest) were handled under water free conditions and used without further purification. Toluene (99.85%, extra dry over molecular sieve) was purchased from Acros Organics. The perfluorinated fluids, Krytox100, Krytox103, and Krytox107, were kindly supplied by Dupont. *n*-Decane, ethanol, *n*-hexadecane, and all the other liquids were purchased from China National Medicines Corporation Ltd.

Growth of SNs: Firstly, the glass slides were treated with piranha solution (H_2O_2:H_2SO_4 = 1:3) at 80 °C for 30 min, rinsed with deionized water, and dried under a nitrogen flow. 8 pieces of the activated glass slides were immersed in 400 mL of toluene with a water concentration of 120 ppm in the custom made chamber. Subsequently, 250 µL of TCMS were injected into the chamber at 25 °C to trigger the growth of SNs. 24 h later, the SNs were successfully grown on the glass slides. The coated samples were rinsed with 10.0 mL of toluene, 10.0 mL of ethanol and 10.0 mL of 50% v/v deionized water/ethanol solution successively, and then dried under a nitrogen flow. In order to change the morphology and density of the SNs, the SNs coated glass slides were repeatedly treated with O_2-plasma at an O_2 flow rate of 10 sccm and a power of 100 W for 5 min (Femto, Germany), and then coated with TCMS according to the above procedure. The samples were designated as SNs1, SNs2, and SNs3 according to the TCMS coating cycles.

Preparation of Fluoro-SNs: Firstly, the SNs coated sample was activated with O_2-plasma at an O_2 flow rate of 10 sccm and a power of 100 W for 5 min. The activated sample was immersed in 75.0 mL of dry toluene, and then 5.0 mL of toluene containing 40.0 µL of PFDTS was added. The sample was kept in the above solution for 24 h at room temperature to ensure complete modification of the SNs. The fluoro-SNs coated glass slide was washed with 10.0 mL of dry toluene and dried under a nitrogen flow.

Preparation of the Fluoro-SNs/Krytox Anti-Wetting Coatings: A certain amount of the Krytox liquid was dropped onto the horizontal fluoro-SNs coated glass slide using a pipette. The fluid spreads quickly and spontaneously on the whole substrate via capillary effect. The sample was kept at room temperature for 10 h to ensure uniform wetting of the surface by the Krytox fluid. The thickness of the Krytox layer in the main text was calculated assuming on a bare glass slide and was controlled by the volume of the Krytox liquid.

Characterization: Measurements of CA and SA were performed with a Contact Angle System OCA 20 (Dataphysics, Germany) equipped with a tilting table. The syringe was positioned in a way that the droplet (10 µL) of liquid could contact surface of the samples before leaving the needle. Tilting angle of the table is adjustable (0–70°) and allows the subsequent measurement of SA at the same position on the sample. The sliding speed was measured using a timekeeper while moving of a liquid droplet on the tilted sample. A minimum of three readings were recorded for each sample. The micrographs of the samples were taken using a field emission scanning electron microscope (SEM, JSM-6701F, JEOL). Before SEM observation, all samples were fixed on aluminum stubs and coated with gold (≈7nm). Transmittance of the samples in 300–800 nm was recorded using a UV-Vis spectrophotometer (Specord 200, Analytik Jena AG).

Supporting Information

Supporting Information is available from the Wiley Online Library or from the author.

Acknowledgements

The authors appreciate financial support from the “Hundred Talents Program of the Chinese Academy of Sciences”.

Received: April 30, 2013
Revised: June 17, 2013
Published online: October 2, 2013

---

[1] a) W. Barthlott, C. Neinhuis, *Planta* **1997**, *202*, 1–8; b) X. F. Gao, L. Jiang, *Nature* **2004**, *432*, 36–36; c) H. Y. Erbil, A. L. Demirel, Y. Avcı, O. Mert, *Science* **2003**, *299*, 1377–1380; d) J. Genzer, K. Efimenko, *Science* **2000**, *290*, 2130–2133; e) L. Jiang, Y. Zhao, J. Zhai, *Angew. Chem. Int. Ed.* **2004**, *116*, 4438–4441; f) N. R. Chiou, C. M. Lu, J. J. Guan, L. J. Lee, A. J. Epstein, *Nat. Nanotechnol.* **2007**, *2*, 354–357; g) J. K. Yuan, X. G. Liu, O. Akbulut, J. Q. Hu, S. L. Suib, J. Kong, F. Stellacci, *Nat. Nanotechnol.* **2008**, *3*, 332–336; h) M. J. Liu, Y. M. Zheng, J. Zhai, L. Jiang, *Accounts. Chem. Res.* **2010**, *43*, 368–377.

[2] a) Z. J. Cheng, L. Feng, L. Jiang, *Adv. Funct. Mater.* **2008**, *18*, 3219–3225; b) E. Hosono, S. Fujihara, I. Honma, H. S. Zhou, *J. Am. Chem. Soc.* **2005**, *127*, 13458–13459; c) F. Shi, Z. Q. Wang, X. Zhang, *Adv. Mater.* **2005**, *17*, 1005–1009; d) Y. Li, L. Li, J. Q. Sun, *Angew. Chem. Int. Ed.* **2010**, *49*, 6129–6133; e) S. M. Kang, I. You, W. K. Cho, H. K. Shon, T. G. Lee, I. S. Choi, J. M. Karp, H. Lee, *Angew. Chem. Int. Ed.* **2010**, *49*, 9401–9404.

[3] A. Steele, I. Bayer, E. Loth, *Nano Lett.* **2009**, *9*, 501–505.

[4] a) H. J. Li, X. B. Wang, Y. L. Song, Y. Q. Liu, Q. S. Li, L. Jiang, D. B. Zhu, *Angew. Chem. Int. Ed.* **2001**, *40*, 1743–1746; b) Q. D. Xie, J. Xu, L. Feng, L. Jiang, W. H. Tang, X. D. Luo, C. C. Han, *Adv. Mater.* **2004**, *16*, 302–305; c) L. Feng, L. Jiang, *Adv. Mater.* **2006**, *18*, 3063–3078; d) J. Zimmerman, M. Rabe, G. J. R. Artus, S. Seeger, *Soft Matter* **2008**, *4*, 450–452; e) T. Darmanin, F. Guittard, *J. Am. Chem. Soc.* **2009**, *131*, 7928–7933.

[5] K. Tsujii, T. Yamamoto, T. Onda, S. Shibuichi, *Angew. Chem. Int. Ed.* **1997**, *36*, 1011–1012.

[6] a) A. Tuteja, W. Choi, M. Ma, J. M. Mabry, S. A. Mazzella, G. C. Rutledge, G. H. McKinley, R. E. Cohen, *Science* **2007**, *318*, 1618–1622; b) X. Deng, L. Mammen, H. J. Butt, Doris Vollmer, *Science* **2012**, *335*, 67–70; c) A. Tuteja, W. Choi, J. M. Mabry, G. H. McKinley, R. E. Cohen, *PNAS* **2008**, *105*, 18200–18205; d) W. C. Wu, X. L. Wang, D.A. Wang, M. Chen, F. Zhou, W. M. Liu, Q. J. Xue, *Chem. Commun.* **2009**, 1043–1045; e) H. X. Wang, Y. H. Xue, J. Ding, L. F. Feng, X. G. Wang, T. Lin, *Angew. Chem. Int. Ed.* **2011**, *50*, 11433–11436; f) S. M. Kang, S. M. Kim, H. N. Kim, M. K. Kwak, D. H. Tahkc, K. Y. Suh, *Soft Matter* **2012**, *8*, 8563–8568.

[7] J. P. Zhang, S. Seeger, *Angew. Chem. Int. Ed.* **2011**, *50*, 6652–6657.

[8] M. J. Liu, S. T. Wang, Z. X. Wei, Y. L. Song, L. Jiang, *Adv. Mater.* **2009**, *21*, 665–669.

[9] T. S. Wong, S. H. Kang, S. K. Y. Tang, E. J. Smythe, B. D. Hatton, A. Grinthal, J. Aizenberg, *Nature* **2011**, *477*, 443–447.

[10] M. Nosonovsky, *Nature* **2011**, *477*, 412–413.

[11] W. Ma, Y. J. Higaki, H. Otsuka, A. Takahara, *Chem. Commun.* **2013**, *49*, 597–599.

[12] a) P. Kim, T. S. Wong, J. Alvarenga, M. J. Kreder, W. E. Adorno-Martinez, J. Aizenberg, *ACS Nano* **2012**, *6*, 6569–6577; b) H. A. Stone, *ACS Nano* **2012**, *6*, 6536–6540; c) A. K. Epstein, T. S. Wong, R. A. Belisle, E. M. Boggs, J. Aizenberg, *PNAS* **2012**, *109*, 13182–13187; d) S. Anand, A. T. Paxson, R. Dhiman, J. D. Smith, K. K. Varanasi, *ACS Nano* **2012**, *6*, 10122–10129.

[13] a) G. Artus, S. Jung, J. Zimmermann, H. P. Gautschi, K. Marquardt, S. Seeger, *Adv. Mater.* **2006**, *18*, 2758–2762; b) J. Zimmermann, F. A. Reifler, G. Fortunato, L. C. Gerhardt, S. Seeger, *Adv. Funct. Mater.* **2008**, *18*, 1–8; c) G. R. Meseck, R. Kontic, G. R. Patzke, S. Seeger, *Adv. Funct. Mater.* **2012**, *22*, 4433–4438; d) J. P. Zhang, S. Seeger, *Adv. Funct. Mater.* **2011**, *21*, 4699–4704.

[14] M. H. Ran, C. X. Yang, Y. Fang, K. K. Zhao, Y. Q. Ruan, J. Wu, H. Yang, Y. F. Liu, *J. Phys. Chem. C* **2012**, *116*, 8449–8455.

[15] a) A. Hozumi, T. J. McCarthy, *Langmuir* **2010**, *26*, 2567–2573; b) K. A. Wier, L. C. Gao, T. J. McCarthy, *Langmuir* **2006**, *22*, 4914–4916; c) C. G. Furmidge, *J. Colloid Sci.* **1962**, *17*, 309–324.

[16] D. F. Cheng, C. Urata, B. Masheder, A. Hozumi, *J. Am. Chem. Soc.* **2012**, *134*, 10191–10199.

[17] D. F. Cheng, C. Urata, M. Yagihashi, A. Hozumi, *Angew. Chem. Int. Ed.* **2012**, *51*, 2956–2959.

[18] I. P. Parkin, R. G. Palgrave, *J. Mater. Chem.* **2005**, *15*, 1689–1695.

[19] M. Masashi, N. Akira, F. Akira, H. Kazuhito, W. Toshiya, *Langmuir* **2000**, *16*, 5754–5760.